Materials Research Express

PAPER

The influence of mechanical activation on the dielectric and dynamic properties and structural parameters of the solid solution of $Pb(Zr_{0.56}Ti_{0.44})O_3$

Materials Research Express

PAPER

The influence of mechanical activation on the dielectric and dynamic properties and structural parameters of the solid solution of $Pb(Zr_{0.56}Ti_{0.44})O_3$

RECEIVED
5 July 2018

REVISED
27 August 2018

ACCEPTED FOR PUBLICATION
4 September 2018

PUBLISHED
14 September 2018

K G Abdulvakhidov[1], M A Sirota[4], A P Budnyk[1], T A Lastovina[1], A V Soldatov[1], S N Kallayev[2], Z M Omarov[2], S A Sadykov[3], B K Abdulvakhidov[3], M A Vitchenko[4], I V Mardasova[4], P S Plyaka[5] and R G Mitarov[6]

[1] The Smart Materials Research Centre, Southern Federal University, Sladkova 178/24, 344090 Rostov-on-Don, Russia
[2] Institute of Physics, Dagestan Research Centre of The Russian Academy of Sciences, Yaragskogo 94, 367003 Makhachkala, Russia
[3] Dagestan State University, Gadjiyeva 43-a, 367000 Makhachkala, Russia
[4] Don State Technical University, Gagarina 1, 344000 Rostov-on-Don, Russia
[5] Southern Scientific Centre of Russian Academy of Sciences, Chekhova 41, 344006 Rostov-on-Don, Russia
[6] Dagestan State Technical University, I. Shamilya 70, 367026 Makhachkala, Russia

E-mail: phys.kam@mail.ru

Keywords: PZT, mechanical activation, debye characteristic temperature, thermal capacity, Debye-Waller factor, mean-square displacement, structural defects

Abstract

The impact of mechanical activation on the dielectric properties, structural parameters, and lattice dynamics of the $Pb(Zr_{0.56}Ti_{0.44})O_3$ solid solution was investigated. The solution features coexisting metastable tetragonal (*T*) and rhombohedric (*R*) phases, whose ratio can be altered by applying the uniaxial compression load up to 320 MPa under torsion in Bridgman anvils. The strain-induced changes of the unit cell parameters, dielectric permittivity, Debye characteristic temperatures, temperature-dependent Debye-Waller factors, and mean square displacements were critically analyzed.

1. Introduction

It is well-known that the physical properties of macroscopic ion crystals depend on the structure of the crystal lattice, the extent of arrangement of atoms and ions in identical crystallographic positions, the type of crystal lattice defects and their concentration. Even a small quantity of defects may influence the phononic and electronic spectra of the crystal lattice, also being manifested in thermodynamic, kinetic and transport properties of the crystal [1]. Intentional tuning of the physical properties by varying the concentration of defects is the actual topics in the condensed matter physics and attracts both theoretical and practical interests.

Among ionic crystalline materials the ferroelectric-piezoelectric solid solutions of $Pb(Zr_{1-x}Ti_x)O_3$ ($0 \leqslant x \leqslant 1$), also known as PZT, with the composition falling around the morphotropic phase boundary (MPB) are of continuous interest due to a wide spectrum of useful physical properties, demonstrating high sensitivity and good stability under the action of an external force [2–6]. By selecting a certain ratio between the Zr^{4+} and Ti^{4+} cations or by introducing some dopants PZT with customized properties can be obtained. Such solid solutions are demanded by the piezoelectric industry for production of functional ceramic elements.

The dielectric, piezoelectric, electromechanic and polarization properties of the $Pb(Zr_{1-x}Ti_x)O_3$ materials with different chemical compositions have been studied under a variety of external forces [7–10]. One of them is a mechanical load applied through the mechanical activation procedure. This external force changes the scale of structural uniformity and concentration of structural defects, affects electric and physical properties, the structural parameters and the lattice dynamics. In this regard establishing the 'composition-structure-properties' correlation is critically important. However, we did not identify any journal publication with detailed analysis about the impact the mechanical force has on PZT. In this work we consider how mechanical activation

influences the dissipative and dynamic characteristics as well as the structural parameters of the $Pb(Zr_{0.56}Ti_{0.44})O_3$ material in form of powder and ceramic by processing the results of its characterization by several experimental techniques such as x-ray diffraction (XRD), dielectric spectroscopy and high-temperature calorimetry.

2. Experimental details

The $Pb(Zr_{0.56}Ti_{0.44})O_3$ samples were prepared in two stages from respective portions of ZrO_2, TiO_2 and PbO of ultra high purity. At the first stage, ZrO_2 and TiO_2 were thoroughly mixed in an agate mortar with addition of ethanol, and then sintered at 1520 K for 2 h. Secondly, the sintered product was grinded and thoroughly mixed with PbO in an agate mortar. The resulting powder was sintered at 1420 K for 2 h in a closed platinum crucible under a layer of $PbZrO_3$. The last is normally used to compensate a partial sublimation of PbO during treatment. The final product was ground into powder in an agate mortar for half an hour. The so-prepared sample will be referred as 'start' one.

The equal weight fractions of the powder were exposed to a fixed mechanical load in Bridgman anvils. To impart the load with some hydrostatic character, the activated powder was confined in a metallic ring, which was positioned between the anvils. The lower anvil was set rotating at a slow angular speed for two full turns with cyclic changes in the direction of rotation. The applied pressures were from 40 to 320 MPa with a 40 MPa step, allowing for generation of structural defects but avoiding intensive amorphization. Each sample was formed by collecting seven portions after the same pressure. Batches were mixed all together in an agate mortar and then sintered at 1420 K for 2 h. Eight different pressures gave eight samples, referred hereafter as 'work' ones.

A characteristic parameter of shear deformation in Bridgman anvils was obtained according to the formula [11]:

$$\zeta = \ln(\upsilon r/d), \tag{1}$$

where υ is the rotational angle, r is the anvil radius, d is the sample thickness.

In our case, $\zeta = 12$, this value remains for all experiments.

The XRD patterns were measured in a step-by-step mode on a HZG-4B x-ray diffractometer with Cu Kα emission in the Bragg-Brentano geometry. Scanning step was 0.01° with counting time of 8 s in each point. The phase purity of the obtained samples was controlled with room temperature measurements and demonstrated no impurities within the sensitivity of the instrument. The refinement of crystal lattice parameters was performed by the method of Rietveld full-profile analysis using the pseudo-Voigt function.

The dynamic characteristics were assessed from the high-temperature measurements of the integral intensities $I_{(110)}$ and $I_{(220)}$ in the paraelectric cubic phase at 773 and 873 K. This method allowed to exclude any impact from the ferroelectric nature of the material as well as from polar directions in the elementary cell manifesting at the phase transition from cubic to ferroelectric. The choice of Bragg reflexes with small Miller indices was due to the weak integral intensities at the large angles of diffraction. The measurement accuracy of temperature control was ±0.5 K; the accuracy of unit cell parameters was ±0.001 Å.

For the following measurements samples were used in form of a 1 mm thick ceramic disc (obtained after sintering). The elemental content of the samples was monitored with the micro x-ray fluorescent spectrometer M4 TORNADO (Bruker). The scan area was 100 × 100 μm^2. The dielectric properties were analysed by using the E7-20 automatic immitance meter produced at the Minsk R&D Institute of Instrument Making. Both sides of the ceramic disc with diameter of 10 mm were covered by a layer of colloidal silver paste and annealed at 1020 K for 20 min to form the conductive pads for electrodes. The samples were measured at 1 kHz frequency. The thermal capacity from ambient temperature to 875 K was evaluated with the DSC 204 F1 Phoenix scanning calorimeter (Netzsch) on the samples in form of the 4 mm diameter discs. The heating rate was 5 K min^{-1} with the measurement accuracy not exceeding 3%.

3. Results and discussion

The elemental composition of Ti and Pb in the resulting samples was found corresponding to the stochiometric one with a 2 wt% discrepancy in the concentration of Pb. This effect is known for lead-containing ferroelectrics and caused by the tendencies of lead oxide to sublime at high temperatures. The difference in concentration of the elements in question was even observed on the surface of $PbTiO_3$ single crystal obtained by crystallization from the melt. The presence of temperature gradient and vaporization of PbO are behind the phenomenon. Long high temperature annealing of such crystals may induce critical changes in their physical and structural properties [12].

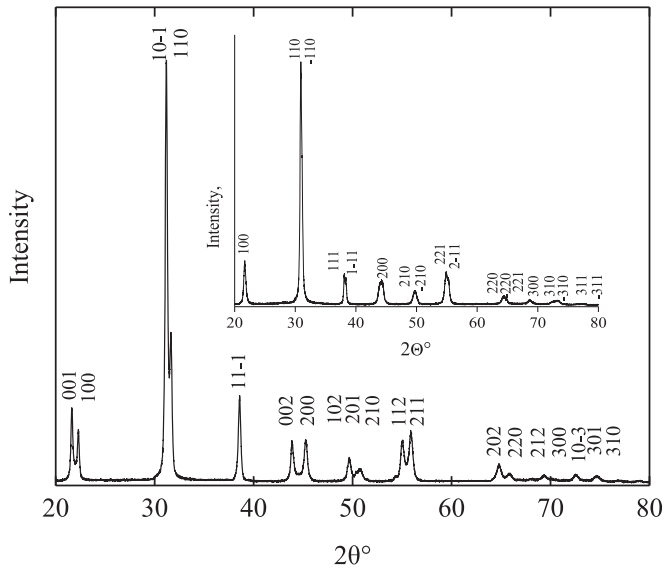

Figure 1. XRD patterns of $Pb(Zr_{0.56}Ti_{0.44})O_3$ before and after (in the inset) applied pressure of 320 MPa.

Table 1. Phase composition of $Pb(Zr_{0.56}Ti_{0.44})O_3$.

	Applied pressure, MPa								
	0	40	80	120	160	200	240	280	320
C_R, %	22	52	86	56	46	52	54	52	76
C_T, %	78	48	14	44	54	48	46	48	24

The XRD patterns of 'start' and 'work' samples after the final pressure of 320 MPa are shown in figure 1. There are two constituent phases can be identified in all the samples; one is the tetragonal *P4mm* phase (*T*-phase) and another is the rhombohedral *R3m* phase (*R*-phase). Their ratio changes from sample to sample, described by relative concentrations of *R*- and *T*-phases, C_R and C_T, respectively (see table 1). The Miller indexes for both phases (*T*-phase for 'start' and *R*-phase for 'work') are given in figure 1 above the patterns. The are no traces of the monoclinous *Cm*-phase observed by other authors [13, 14].

It is typical of ferroelectric materials exposed to mechanical stress in Bridgman anvils to display some structural changes like accumulated dislocations and point defects. These defects can be easily traced through the changes in size of coherent scattering regions, *D*, micro deformations, $\Delta d/d$ (where *d* is the interplanar distance), and the integral intensities of the diffractive profiles [15–17]. Figure 2 shows *D* and $\Delta d/d$ values (united with polynomical eyeguides simulated using the Modified Bezier method) for $Pb(Zr_{0.56}Ti_{0.44})O_3$ after mechanical activation at different pressures, P, (figure 2(a)) and sucessive sintering (figure 2(b)).

As can be seen from figure 2(a), while the applied pressure increases till 160 MPa *D* decreases and $\Delta d/d$ changes non-monotonically. The stress of 160 MPa can be considered as 'critical' for the system, since above this value the development of dislocations slows down, while the generation of point defects becomes dominant in formation of the structural defects.

The ballistic diffusion processes developing in the sample confined in Bridgman anvils under applied mechanical stress exceeding some 'critical' value lead to recrystallization. At certain stage of such mechanical activation under a constant value of shear deformation some defective crystallities get consumed by less defective ones promoting the growth of 'healthy' crystallites and *D* values [18]. This process appears under the pressures of 200 and 280 MPa as in figure 2(a).

The complex character of the $\Delta d/d$ behavior over the course of mechanical activation (figure 2(a)) can be partially attributed to the double-phase nature of $Pb(Zr_{0.56}Ti_{0.44})O_3$ composition adjoining from the left MPB at the *x*–*T* phase diagram, where *x* is the concentration of Ti^{4+} ions, *T* is the phase transition temperature [2, 3]. It is well established, that PZT with exact composition is quite sensitive to any external force, e.g. to the mechanical pressure [9, 10, 16, 17, 19–22].

Mechanical activation is characterized by a certain correspondence between the values of applied pressure and the induced concentrations of structural defects such as dislocations and point defects. The number of point defects was not evaluated in this work, and they will be described qualitatively. Considering the dislocations, the

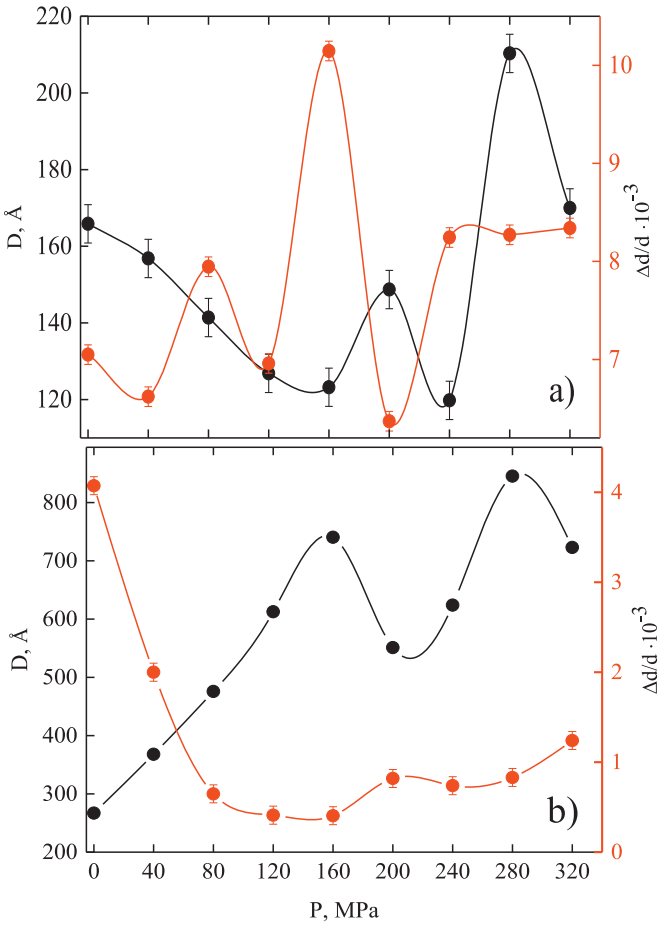

Figure 2. Changes in the size of coherent scattering regions (D) and micro deformations ($\Delta d/d$) in $Pb(Zr_{0.56}Ti_{0.44})O_3$ samples induced by mechanical activation (a) and by successive thermal treatment (b).

Table 2. Density of dislocations in $Pb(Zr_{0.56}Ti_{0.44})O_3$ during mechanical activation before and after calcination.

ρ_D	Applied pressure, MPa								
10^{11} cm^{-2}	0	40	80	120	160	200	240	280	320
Before	11	12	15	19	20	14	21	7	10
After	0.4	1.2	3.3	4.3	4.4	2.8	3.1	2.8	2

contribution of screw dislocations into the widening of diffraction profiles is virtually negligible, and one deals mainly with edge dislocations. Hence, the density of dislocations, ρ_D, can be estimated by using the following formula [23]:

$$\rho_D = 3nD^{-2}, \tag{2}$$

where $n = 1$, assuming, that dislocations network coincides with grains boundaries and large separations imply almost no interaction between the dislocations.

The estimated ρ_D values for the samples before and after calcination are presented in table 2.

Figure 3 shows the changes of the unit cell parameters for *T*- and *R*-phases with rising applied pressure. It is clear that a_R deviates more than both a_T and c_T parameters. This can be attributed to the fact that *R*-phase features eight probable equivalent polar directions for orientation of the vector of spontaneous polarity, *Ps*. The *T*-phase has only six probable directions. The coercive field is minimal in the morphotropic region, implying the increase of the reorientational component of polarization. In $Pb(Zr_{0.56}Ti_{0.44})O_3$ the 180° and 90° domain structures are typical for *T*-phase while the 180° and 109° (71°) are for *R*-phase. The pressure-induced switching of the 90° domains in *T*-phase is difficult due to the strains in incoherent interphase boundaries of the linked 90° twins. The substantial changes in the a_T and c_T parameters are observed above 200 MPa. With growing pressure the crystal lattice of *T*-phase starts to shrink along *c*-axis and extends along axes *a* and *b* (the unit cell parameter *a*

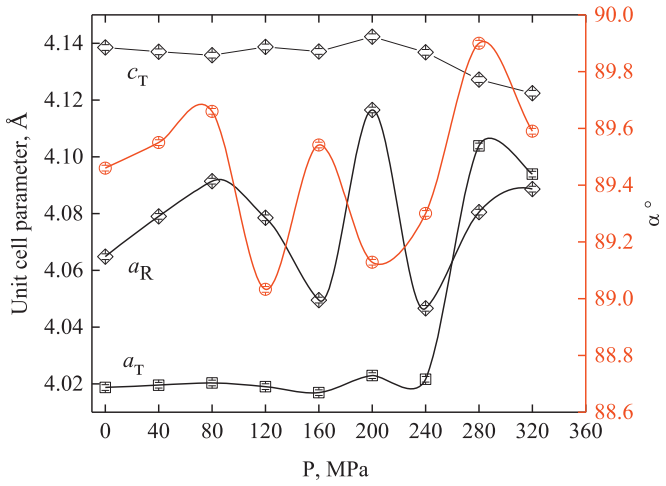

Figure 3. The unit cell parameters in *T*-phase (a_T, c_T) and *R*-phase (a_R) and the rhombohedral angle (α) in the $Pb(Zr_{0.56}Ti_{0.44})O_3$ samples after different applied pressures.

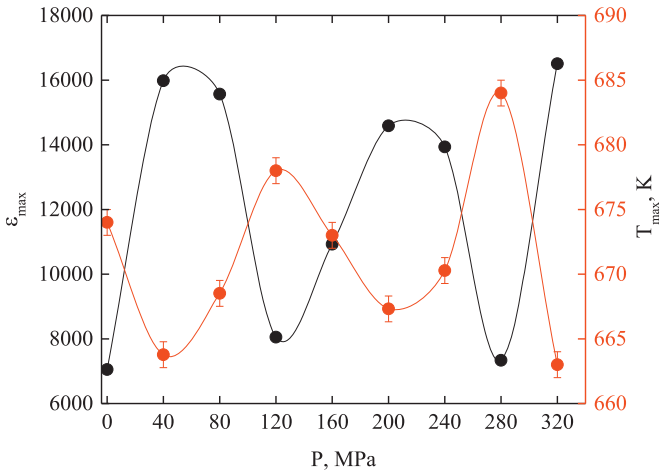

Figure 4. Dependence of the dielectric permittivity ε_{max} and temperature T_{max} for $Pb(Zr_{0.56}Ti_{0.44})O_3$ ceramics on the applied mechanical pressure.

equals *b* for *T*-phase). At pressures higher than reported in this work, there is a possibility for formation of metastable phases with another spatial symmetry and unit cells. The rhombohedral angle, α, is another characteristic parameter for the *R*-phase unit cell. Its value oscillates as the a_R parameter under mechanical activation (figure 3).

Let us discuss the behavior of dielectric permeability, ε, which is one of the fundamental parameters of ferroelectrics. Previously, we obtained the dependencies of ε from temperature and frequency for a couple of 'start' and 'work' samples [24]. In this study we will focus on dependencies of ε_{max} and T_{max} from the activation pressure, shown in figure 4. Both values oscillate in a wide interval. The ferroelectic ceramics ε_{max} depends on such factors as grain size, domain structure, and density of material. The mean density of the samples was 96% of its theoretical value.

In the $Pb(Zr_{0.56}Ti_{0.44})O_3$ solid solutions thermal motion of ions could lead to their displacement from equilibrium in the crystal lattice. The applied mechanical pressure may cause a static shift. Both dynamic and static shifts result in lower intensities of diffractograms due to higher number of ions situated in 'dislocated' sites of the crystal lattice. The measure of the shift is the root-mean-square amplitude, $\bar{U}^2$, which can be determined for the crystals of cubic syngony via the following relationships:

$$\overline{U^2} = \frac{3a^2}{4\pi^2[(h_2^2 + k_2^2 + l_2^2) - (h_1^2 + k_1^2 + l_1^2)]} \cdot \ln\left[\left(\frac{I_1}{I_2}\right)_{start} \cdot \left(\frac{I_2}{I_1}\right)_{work}\right], \quad (3)$$

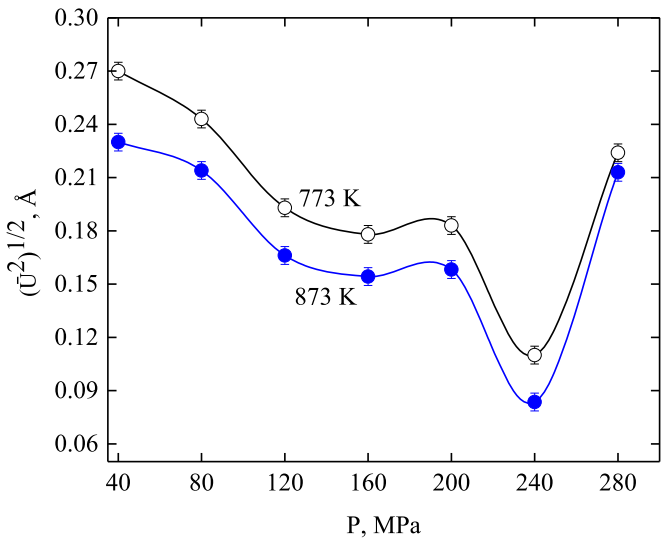

Figure 5. Dependence of squared-mean static shift on the applied pressures for the $Pb(Zr_{0.56}Ti_{0.44})O_3$ samples. The $(\overline{U}^2)^{1/2}$ values were calculated from XRD patterns measured on samples at 773 and 873 K.

where a is the unit cell parameter, hkl are the Miller indices, I_1 and I_2 are the integral intensities from the (110) and (220) reflecting planes of 'start' and 'work' samples, respectively.

The integral intensities were obtained from the XRD measurements on samples heated at 773 and 873 K. At these temperatures $Pb(Zr_{0.56}Ti_{0.44})O_3$ has the cubic phase, because remains away from the temperature of phase transition, T_m. The calcualted squared-mean shift $(\overline{U}^2)^{1/2}$ values are shown in figure 5 from where it comes clear that growing mechanical stess causes similar changes in sample after each activation temperature. The diffusion processes occur intensively under heating at a high temperature and result in a partial 'dissipation' of structural defects restoring the crystal lattice, what is reflected by growing D and decreasing $\Delta d/d$ (see table 1 and figure 2(b)).

To calculate the lattice dynamics of cubic crystal, we adopted the Debye model [25]. At first approximation it assumes that crystal behaves as an isotropic continuous solid body, where all the waves travel at the same speed irrespective of wavelength or direction. We will consider the behaviour of the characteristic temperature, Θ, as a measure of the interatomic bonds strength under applied mechanical pressure. In the Debye approximation, it is given by

$$h\nu_m = k\Theta, \tag{4}$$

where ν_m is the frequency of the upper limit of vibration spectrum, k and h are the Boltsmann and Planck constants, respectively.

In order to define the characteristic temperature of thermal motion of the ions in the cubic phase lattice we will use the measured at 773 and 873 K the integral intensities of the (220) reflection from $Pb(Zr_{0.56}Ti_{0.44})O_3$.

$$\ln\frac{I_{T773}}{I_{T_{873}}} = \frac{6h^2}{mk\Theta}\frac{\sin^2\vartheta}{\lambda^2}\left[\frac{\Phi\left(\frac{\Theta}{T_{873}}\right)}{\frac{\Theta}{T_{873}}} - \frac{\Phi\left(\frac{\Theta}{T_{773}}\right)}{\frac{\Theta}{T_{773}}}\right], \tag{5}$$

where m is the reduced mass of atoms in the unit cell, $\Phi\left(\frac{\Theta}{T}\right)$ is the tabulated Debye function, ϑ is the angle of diffraction, λ is the x-ray wavelength.

By considering the ratio of intensities $\frac{I_{T773}}{I_{T873}}$, we will find

$$\alpha = \frac{1}{\Theta}\left[\frac{\Phi\left(\frac{\Theta}{T_{873}}\right)}{\frac{\Theta}{T_{873}}} - \frac{\Phi\left(\frac{\Theta}{T_{773}}\right)}{\frac{\Theta}{T_{773}}}\right] = \frac{\lambda^2}{\sin^2\vartheta}\frac{mk}{6h^2}\cdot\ln\frac{I_{T_{773}}}{I_{T_{873}}}. \tag{6}$$

After calculating α, we can find the Debye characteristic temperature, Θ, by using a reference curve $\alpha = f(\Theta)$ [26, 27], which was constructed for both temperatures.

The resulting dependence $\Theta = f(P)$ is presented in figure 6. There are no appreciable changes in Θ for activation pressures below 80 MPa. Within this interval, dislocations get concentrated and the blocks of crystalline mosaic become smaller. Pressures of 120 and 160 MPa correspond to the beginning of the active

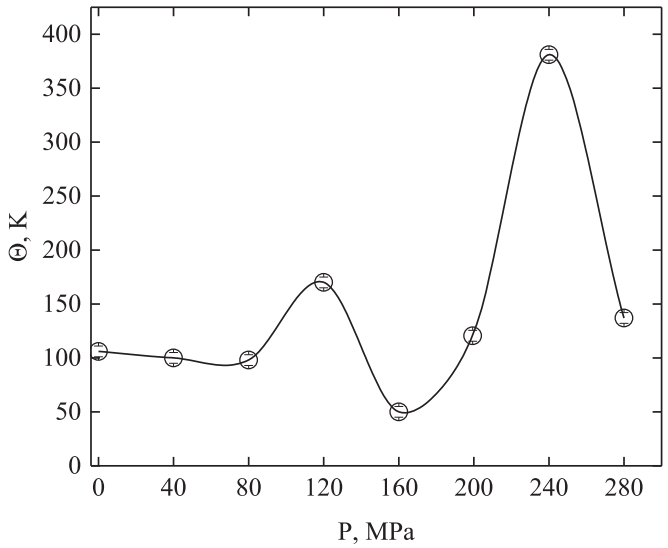

Figure 6. Dependence of the Debye characteristic temperature of $Pb(Zr_{0.56}Ti_{0.44})O_3$ on the applied mechanical pressure.

generation of point defects and maximal concentration of dislocations, respectively. The 240 MPa activation pressure corresponds to the highest values of Θ and concentration of *T*-phase among the activated samples, and to the lowest values of *D* and $\bar{U}^2$ (see figures 6, 2(a) and 5).

Metal ions in the vicinity of a dislocation or point defect should scatter x-rays in the same manner as they are scattered by the ions shifted from the equilibrium by a heat movement due to substantial deviations from the mean positions in the crystal lattice of $Pb(Zr_{0.56}Ti_{0.44})O_3$ that abruptly decreases with the distance from a dislocation. The x-rays scattered by shifted ions do not coincide in phase, causing the weakening of intensity of diffraction peaks. This lowering of the intensity is described by the equation:

$$\frac{I_T}{I} = e^{-2M}, \tag{7}$$

where *I* is the intensity of reflected x-ray (without considering thermal vibrations), I_T is the true intensity, e^{-2M} is the Debye-Waller isotropic thermal factor.

$$I_T = Ie^{-2M} = e^{-2B}\left(\frac{\sin\vartheta}{\lambda}\right)^2. \tag{8}$$

The *B* value is calculated using

$$B = \frac{6h^2}{mk\Theta}\left[\frac{\Phi(x)}{x} + \frac{1}{4}\right], \tag{9}$$

where $x = \Theta/T$; $\Phi(x)/x$ is the Debye function; 1/4 is the share of zero vibrations.

The results of calculation of *B* can be seen in figure 7.

It is well known from thermodynamics, that first-order phase transitions involve the transfer of a latent heat. Figure 8(a) presents a thermal dependence of the thermal capacity of ceramic polycrystalline samples produced from the starting (1) and activated powders at 80 (2) and 160 (3) MPa applied pressures. According to [28], the high concentration of defects leads to an increase in thermal capacity and blurring of the heat capacity jump when approaching the phase transition point. The same behavior was observed during the experiment. For the analysis of thermal capacity and for distinquishing the phononic and abnormal inputs we will use the same to [28, 29], a simple model that describes the phononic thermal capacity of PZT by using the Debye function of $C^0{}_p \sim D(\Theta_D/T)$, where Θ_D is the qualitative (calorimetric) Debye temperature. The results of thermal capacity indicate that the Debye temperature for the starting (1) and work samples, which experienced mechanical activation at 80 (2) and 160 (3) MPa before heating, are equal to $\Theta_D =$ 566, 561 and 550 K respectively. These values exceed the qualitative temperatures of the powdered samples described above.

It is known that the Debye temperature depends on the value of the coupling forces between the lattice atoms, therefore, the temperature drop under power impact may reflect the weakening of the forces among the lattice ions. The results of the phononic thermal capacity approximation by applying the Debye function are shown as a continuous line in figure 8(a).

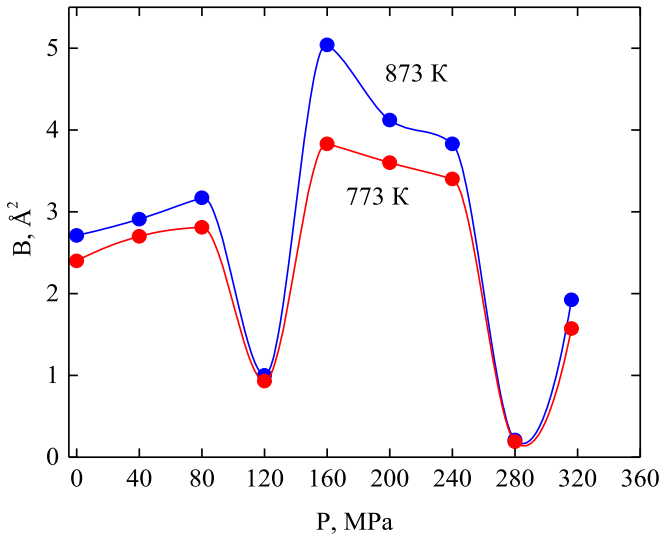

Figure 7. Dependence of the Debye-Waller factor of $Pb(Zr_{0.56}Ti_{0.44})O_3$ powders on mechanical activation pressure.

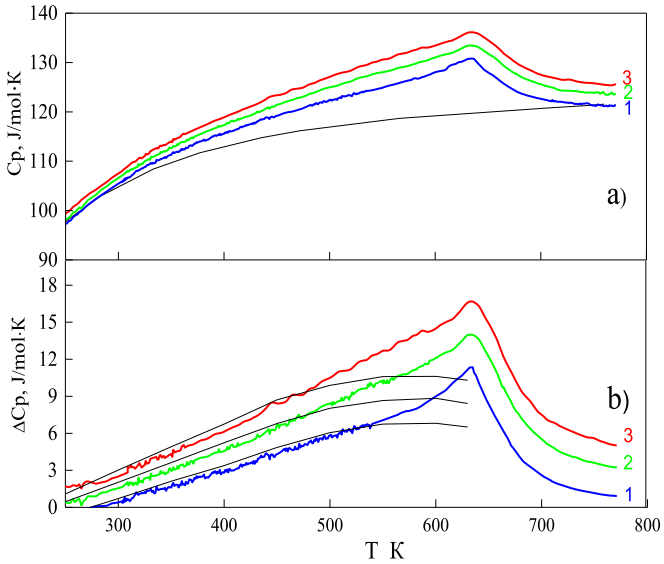

Figure 8. Thermal dependence of the heat capacity of $Pb(Zr_{0.56}Ti_{0.44})O_3$ (a) and of the abnormal thermal capacity $\Delta C(T)$ of $Pb(Zr_{0.56}Ti_{0.44})O_3$ ceramics obtained from the starting (1) and activated powders at 80 (2) and 160 (3) MPa pressures.

The thermal capacity surplus constituent was established for each composition as the difference between the measured and estimated phononic thermal capacities $\Delta C = C_P - C^0{}_P$. The thermal dependence of the abnormal thermal capacity $\Delta C(T)$ is presented in figure 8(b).

Thus the nature of the highlighted thermal capacity enables to interpret it as a Schottki anomaly for twin-layer conditions divided with energy barrier ΔE. They could be considered as domains separated by the energy barrier, ΔE, or as the atoms of the same type or even the groups of atoms having two structurally equivalent positions [30].

The Schottki thermal capacity expression for the twin-layer model is given below [31]:

$$\Delta Cp = \frac{R[G(\Delta E/kT)^2 \exp(-\Delta E/kT)]}{[1 + G\exp(-\Delta E/kT)]^2}, \quad (10)$$

where G is the relation of the degeneracy multiplicity of the layers, R is the absolute gas constant.

By comparing the thermal capacity calculated using equation (10) and the experimentally highlighted abnormal thermal capacity ΔC we have obtained the model parameters for the samples (1) $E = 1.391$ eV; $G = 1.767$; (2) $E = 1.511$ eV; $G = 3.177$; (3) $E = 1.575$ eV; $G = 4.611$. A good match between the experimentally highlighted $\Delta C(T)$ and the estimated curve of the abnormal thermal capacity dependence within

a 250–550 K range is rather good (figure 8). In the region of the ferroelectric phase transition, T_c, one can observe a typical λ-abnormality of thermal capacity $C_p(T)$, which is due to the onset of ferroelectric alignment. T_{max} temperature being determined by dielectric measurements may not coincide with the maximal parameters of non-electric measurements. e.g. calorimetric ones.

4. Conclusions

The sum of the experimental results enables us to conclude that mechanical activation at room temperature of the $Pb(Zr_{0.56}Ti_{0.44})O_3$ powder with composition from MPB trigger the processes of relaxation of mechanical energy through dispersion of original crystallites and accumulation of structural defects that influence not only the structural parameters and the crystal lattice dynamics but the ratio of coexisting *R*- and *T*-phases. The $Pb(Zr_{0.56}Ti_{0.44})O_3$ ceramic with a variety of structural defects features different values of dielectric permeability, temperature of the dielectric permeability maximum, and the thermal capacity in MPB.

Funding

Authors acknowledge the Grant of the Southern Federal University (VnGr-07/2017-08) for the financial support.

ORCID iDs

K G Abdulvakhidov https://orcid.org/0000-0001-6697-9192

References

[1] Maradudin A 1968 *The Defects and The Vibration Spectrum of Crystals* (Moscow: MIR)
[2] Jaffe B, Cook W R and Jaffe H 1971 *Piezoelectric Ceramics* (London: Academic)
[3] Smazhevskaya E G and Feldman N B 1971 *Piezoceramics* (Moscow: Sovetskoye Radio)
[4] Soares M R, Senos A M R and Mantas P Q 2000 Phase coexistence region and dielectric properties of PZT ceramics *J Eur. Ceram. Soc.* **20** 321
[5] James N K, Lafont U, van der Zwaag S and Groen W A 2014 Piezoelectric and mechanical properties of fatigue resistant, self-healing PZT–ionomer composites *Smart Mater. Struct.* **23** 055001
[6] Van Loock F, Deutz D B, van der Zwaag S and Groen W A 2016 Exploring the piezoelectric performance of PZT particulate-epoxy composites loaded in shear *Smart Mater. Struct.* **25** 085039
[7] Averin I A and Pecherskaya P M 2006 Control of the properties of $Pb(Zr_{1-x}Ti_x)O_3$ solid solutions by external interference *Solid State Phys.* **48** 1096
[8] Zhakharov Y N, Rayevskaya S I, Borodin V Z, Kouznetsov V G and Rayevsky I P 2006 Controlling the values of thermal hysteresis and degradation of the dielectric Anomaly in the region of ferro-antiferroelectric phase transition in $Pb(Zr_{1-x}Ti_x)O_3$ ($0.03 \leqslant x \leqslant 0.05$) Ceramics *Solid State Phys.* **48** 1077–8
[9] Frantti J, Fujioka Y, Zhang J, Wang S and Vogel S C 2012 High-pressure neutron study of the morphotropic lead-zirconate-titanate: phase transition in a two-phase system *J Appl. Phys.* **112** 014104
[10] Frantti J, Fujioka Y, Zhang J, Zhu J, Vogel S C and Zhao Y 2014 Microstrain in tetragonal lead-zirconate-titanate: the effect of pressure on the ionic displacements *Rev. Sci. Instrum.* **85** 083901
[11] Valiev R Z and Alexandrov I V 2000 *Nanostructural Products of Intense Plastic Deformation* (Moscow: Logos)
[12] Kupriyanov M, Kovtun D, Zakharov A, Kushlyan G, Yagunov S, Kolesova R and Abdulvakhidov K 1998 Summary data on ferroelectric $PbTiO_3$ structure *Ph. Trans.* **64** 145
[13] Noheda B, Cox D E, Shirane G, Gonzalo J A, Cross L E and Park S-E 1999 A monoclinic ferroelectric phase in the $Pb(Zr_{1-x}Ti_x)O_3$ solid solution *Appl. Phys. Lett.* **74** 2059
[14] Noheda B 2002 Structure and high-piezoelectricity in lead oxide solid solutions *Curr. Opin. Solid St.* M **6** 27
[15] Abdulvakhidov K G, Vitchenko M A, Mardasova I V and Oshaeva E N 2008 Properties of the ferroelectric ceramics fabricated from an ultradispersed powder *Tech. Phys.* **53** 661
[16] Ubushaeva E N, Abdulvakhidov K G, Mardasova I V, Abdulvakhidov B K, Vitchenko M A, Amirov A A, Batdalov A B and Gamzatov A G 2010 Nanostructured multiferroic $PbFe0_{.5}Nb_{0.5}O_3$ and its physical properties *Tech. Phys.* **55** 1596
[17] Abdulvakhidov K G *et al* 2016 Phase transitions, magnetic and dielectric properties of $PbFe_{0.5}Nb_{0.5}O_3$ *Ferroelectrics* **494** 182
[18] Okadzaki K 1976 *Ceramic Dielectric Technology* (Moscow: Energy)
[19] Sirota M A and Abdulvakhidov K G 2017 Mechanical activation and electrophysical properties of $Pb(Zr_{0.58}Ti_{0.42})O_3$ *J. Surf. Invest.: X-Ray, Synchrotron Neutron Tech.* **11** 677
[20] Saley V A, Ponomaryev Y A, Klimov V V and Poplavko Y M 1978 X-ray study of PZT solid solutions in the tetragonal-rhombohedral phase transition composition area *Ferroelectrics* **22** 805
[21] Amin A, Newnham R E and Cross L E 1986 Effect of elastic boundary conditions on morphotropic $Pb(Zr, Ti)O_3$ *Phys. Rev.* B **34** 1595
[22] Turik A V 1986 On the nature of the morphotropic transition in ferroelectric systems *Kristallografiya* **26** 171
[23] Vasil'ev D M and Smirnov B I 1961 Certain X-RAY diffraction methods of investigating cold worked metals *Sov. Phys. Usp.* **4** 226
[24] Sirota M A *et al* 2018 Mechanical activation and physical properties of $Pb(Zr_{0.56}Ti_{0.44})O_3$ *Ferroelectrics* **526** 1
[25] Kittel C 1978 *Introduction to Solid State Physics* (Moscow: Nauka)
[26] Mirkin L I 1961 *Guide to X-ray Structural Analysys of Polycrystals* (Moscow: Physics-Mathematics Literature Press)
[27] James P 1950 *Optical Principles of X-ray Diffraction* (Moscow: Inostrannaya Literatura)
[28] Mitarov R G, Kallaev S N, Omarov Z M and Abdulvakhidov K G 2015 Thermal capacity of $PbFe_{0.5}Nb_{0.5}O_3$ multiferroic *Solid State Phys.* **57** 710

[29] Levanyuk A P, Osipov V V, Sigov A S and Sobyanin A A 1979 Change of defect structure and the resultant anomalies in the properties of substances near phase-transition points *Sov. Phys. JETP* **49** 176
[30] Yakushev E D 2004 Thermal conductivity of SBN ferroelectric-relaxor *Solid State Phys.* **46** 325
[31] Zhouze V P 1973 *Physical Properties of Rare-Earth Chalcohenide* (Leningrad: Nauka)